Advances in Computational Design, *Vol. 2, No. 1 (2017) 43-56*
DOI: https://doi.org/10.12989/acd.2017.2.1.043

Determination of bearing type effect on elastomeric bearing selection with SREI-CAD

Barbaros Atmaca* and Sevket Ates[a]

Karadeniz Technical University, Department of Civil Engineering, 61080 Trabzon, Turkey

(Received June 15, 2016, Revised October 26, 2016, Accepted November 3, 2016)

Abstract. The aim of this paper is to develop software for designing of steel reinforced elastomeric isolator (SREI) according to American Association for State Highway and Transportation Officials Load and Resistance Factor Design (AASHTO LRFD) Specifications. SREI is used for almost all bridge types and special structures. SREI-structures interface defines support boundary conditions and may affect the seismic performance of bridges. Seismic performance of the bridge is also affected by geometrical and materials properties of SREI. The selection of SREI is complicated process includes satisfying all the design constraints arising from code provisions and maximizing performance at the lowest possible cost. In this paper, design stage of SREI is described up to AASHTO LRFD 2012. Up to AASHTO LRFD 2012 analysis and design program of SREI performed different geometrical and material properties are created with C# object-oriented language. SREI-CAD, name of the created software, allows an accurate design for economical estimation of a SREI in a short time. To determine types of SREI effects, two different types of bearings, rectangular and circular with similar materials and dimension properties are selected as an application. Designs of these SREIs are completed with SREI-CAD. It is seen that ensuring the stability of circular elastomer bearing at the service limit state is generally complicated than rectangular bearing.

Keywords: C# programming language; steel reinforced elastomeric isolator; software engineering

1. Introduction

Bridges and viaducts are one of the most important components of transportation network of this era. Especially in the seismic zone of the world, in order to prevent the interruption of transportation network after the earthquakes, these structures have to be protected from hazardous effects of earthquakes. For this purpose several methods are developed to protect these structures. One of the most notable techniques among them is isolation system. Thanks to isolation system, interaction between the structure and soil is reduced. This ensures to decrease the acceleration transmitted to the structure by the earthquake. There are two basic types of isolation systems; one of which uses elastomeric and the other one uses sliding system. Steel reinforced elastomeric isolation (SREI) is a type of elastomeric isolation system. SREI consists of thin layers of natural or synthetic rubber such as polychloroprene bonded to steel plates. This structure of SREI provides

*Corresponding author, Ph.D., E-mail: atmaca@ktu.edu.tr
[a]Associate Professor, E-mail: sates@ktu.edu.tr

http://www.techno-press.com/journals/acd&subpage=7 ISSN: 2383-8477 (Print), 2466-0523 (Online)

sufficient vertical rigidity and allows horizontal flexibility to shift the fundamental frequency of an isolated structure away from the dominant frequency range of most earthquakes (Moon, Kang *et al*. 2002, Dookie, Ju *et al*. 2013).

Although SREI have been widely used throughout the United States and Europe since the 1950's, the first recorded use of neoprene bearing pads in the United States was to support prestressed concrete beams in Victoria, Texas in 1957 (Muscarella 1995). From introduction of elastomeric bearing to today codes have widely changed depending on researches. The first AASHTO Standard Specifications for Highway Bridges to address elastomeric bearings was the 8th Edition, published in 1961 and consisted of only one page of details governing their use. Roeder, Stanton *et al*. (1987) their NCHRP Project included an extensive series of laboratory tests on elastomeric bearings of all shapes and sizes. The final result of the test program was to give a choice of two design methods, a simple restrictive one, (Method A), and another (Method B) based more on theoretical calculations which required additional testing of the elastomer so that its material properties would be well defined. Buckle and Kelly (1986) studied the stability of elastomeric bearings using a model bridge deck tested using a shaking table. Bearing overturning or rollover was evident in these tests, since the bearings were doweled. Harper and Consolazio (2013) emphasized that accurate estimates of bearing stiffnesses are often necessary for bridge design and construction calculations. Yazdani, Eddy *et al*. (2000) stated that the stiffness of elastomeric bearing correctly calculated accordance with AASHTO. Green, Yazdani *et al.* (2007) emphasized that elastomeric bearing were frequently used prestressed girder highway bridges and boundary conditions between bridge girder and elastomeric bearing have an effect on seismic performance of bridges. Akoglu and Celik (2008) focused on the effect of design phase of elastomeric bearing on dynamic characteristic of bridge. For this purpose, changes in period and internal forces of the bridge depending on the mechanical properties of different types of rubber bearings were compared. Olmos and Roesset (2010) investigated the effects of the nonlinear behavior of the isolation pads on the seismic response of bridges with rubber bearings Manos, Mitoulis *et al*. (2011) created software for preliminary design of seismically isolated R/C highway overpasses is based on the current design provisions of Eurocode 8 (Part 2) as well as on engineering decisions included in the expert system. Atmaca, Yurdakul *et al*. (2012) emphasized that usage of the isolation devices offers some advantages for the internal forces on the deck for the considered isolated bridge as per the non-isolated bridge. Melkumyan (2013) dedicated to the design of high damping laminated rubber-steel bearings. Patrick, Azlan *et al.* (2014) investigated the seismic performance of low-rise precast wall system with high damping rubber bearing. Danielle, Mariacristina *et al*. (2014) defined of optimal design parameters characterizing the isolation system of a bridge, both in the case of elastomeric and sliding bearings, having viscoelastic or rigid-plastic behavior, respectively, installed between the piers and the deck. Forcellini and Kelly (2014) worked on analysis of the large deformation stability of elastomeric bearings. Islam, Hussain *et al*. (2014) demonstrated that the values of the FEM-based structural design parameters are greatly reduced when the isolator is used. Jian, Xiaohong *et al.* (2015) described Optimum design of lead-rubber bearing system with uncertainty parameters. Chen *et al.* (2016) have investigated the effectiveness of LRBs in framed underground structures on controlling structural seismic responses.

As it is seen in literature, studies show significance of elastomeric bearings for dynamic characteristic of structures. Insofar as elastomeric bearings have been in wide spread use throughout the world with great success, accurate design of SREI is getting vitally important. In this study, design stage of SREI is explained according to AASHTO LRFD (2012). Software

(SREI-CAD) is written by using C# programming language to perform accurate design stage and an economical estimation of SREI in short time. To determine types of SREI effects, two different types of bearings, rectangular and circular with similar materials and dimension properties are selected as an application. Designs of these SREIs are completed with SREI-CAD which has capability for designing of SREI, both rectangular and circular in shape.

2. SREI design

The design phase of SREI is taken into account according to the AASHTO LRFD (2012)-Section 14 which refers to the basic requirements and compliance criteria, analysis procedures and the verification of the isolation system. AASHTO LRFD is prescribed two design method referred to as Method A and Method B for SREI. For large bearing bigger than 20.32 cm thicknesses or 6.45 cm^2 surface area, Method B is recommended to use. Therefore, parameters of Method B are taken account in this study.

2.1 Bearing dimensions and components

SREI shall consist of alternate layers of steel reinforcement and rubber bonded together. According to plan view elastomeric bearing is divided into two groups as a rectangular and circular. Fig. 1 shows a plan view and cross section of a rectangular elastomeric bearing.

Two factors limit the maximum compressive stress allowed on the bearing: compressive deformation and shears strains which result from compression. The first factor is the compressive deformation of the bearing, most of which results from the bulging of the elastomer under compressive load. There is actually very little volume change in elastomeric materials of lower hardness ratings but, as the hardness of the elastomer increases, the volume change of the material becomes more significant. This tendency to bulge under compressive load can be described by a quantity known as the shape factor, S, the ratio of the loaded plan area, divided by the area free to bulge (Muscarella 1995). In other words, the shape factor is a ratio of restrained area to unrestrained surface areas. In practice, the shape factor is used to try to capture the effect of

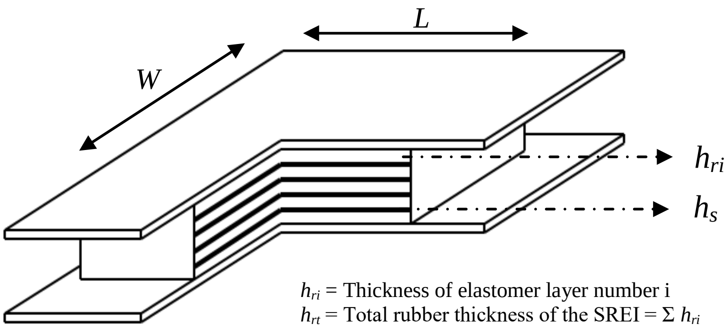

h_{ri} = Thickness of elastomer layer number i
h_{rt} = Total rubber thickness of the SREI = $\Sigma\ h_{ri}$
h_s = Thickness of reinforcing steel plate
W = Width of SREI
L = Length of SREI

Fig. 1 Elastomeric bearing

geometry of the elastomeric layer on compression, and shear capacity of bearing. For rectangular bearings without holes, the shape factor of a layer may be taken as

$$S_i = \frac{LW}{2h_{ri}(L+W)} \tag{1}$$

For circular bearings without holes, the shape factor of a layer may be taken as

$$S_i = \frac{D}{4h_{ri}} \tag{2}$$

where D diameter of circular SREI.

2.2 Material properties

The design of SREI requires a balance between the stiffness required to support large compressive load and the flexibility needed to accommodate translation and rotation. The balance is maintained by using a relatively flexible elastomer with a shear modulus, G, between 0,55 MPa and 1,25 MPa (80 and 180 psi) and an appropriate shape factor (AASHTO LRFD). Horizontal (K_H) and vertical stiffness (K_V) of the SREI is calculated to assume rubber and steel part of bearing have elastic behavior. The rotational stiffness of SREI (K_θ) as a result of the rotational behavior of a simple beam is computed as follows

$$K_H = \frac{GA}{h_{rt}}, \; K_V = \frac{EA}{h_{rt}}, \; K_\theta = \frac{1,6(0,5EI)}{h_{rt}} \tag{3}$$

One of the most important material properties used in the design of the elastomeric bearing is the elastic modulus (E). Elastic modulus of elastomeric bearing may be obtained as follows

$$E=4,8GS^2 \tag{4}$$

2.3 Design requirements

2.3.1 Shear deformations

The maximum shear deformation of the bearing, at the service limit state, Δ_S, is limited to ±0.5 h_{rt} in order to avoid rollover at the edges and delamination due to fatigue.

2.3.2 Combined compression, rotation, and shear

SREI is almost incompressible, so when it is loaded in compression, the rubber expands laterally due to the Poisson effect. That expansion is partially restrained by the steel plates to which the rubber layers are bonded, and the restraint results in bulging of the layers between the plates. The bulging creates shear stresses at the bonded interface between the rubber and steel. If they become large enough, they can cause shear failure of the bond or the rubber adjacent to it. This is the most common form of damage in SREI and is the reason why limitations on the shear strain in the rubber dominate the design requirements (AASHTO LRFD 2012).

Combinations of axial load, rotation, and shear at the service limit state are permitted by Method-B as follow

$$(\gamma_{a,st}+\gamma_{r,st}+\gamma_{s,st})+1,75(\gamma_{a,cy}+\gamma_{r,cy}+\gamma_{s,cy})\leq 5,0 \text{ and } \gamma_{a,st}\leq 3,0 \tag{5}$$

Where γ_a is shear strain caused by axial load; γ_r shear strain caused by rotation; γ_s shear strain caused by shear displacement. Subscripts "*st*" and "*cy*" indicate static and cyclic loading, respectively.

2.3.3 Stability of SREI

The stability of SREI is investigated at the service limit state load combinations. SREI satisfying shall be considered stable, and no further investigation of stability is required. Otherwise circular SREI is considered instable but there is an additional investigation for stability of rectangular SREI

$$A=\frac{1,92\frac{h_{rt}}{L}}{\sqrt{1+\frac{2,0L}{W}}},\quad B=\frac{2,67}{(S_i+2,0)\left(1+\frac{L}{4,0W}\right)} \tag{6}$$

For rectangular SREI not satisfying requirement of 2A≤B, the stress due to the total load shall satisfy following equation.

If the bridge deck is free to translate horizontally

$$\sigma_s\leq\frac{GS_i}{2A-B} \tag{7}$$

If the bridge deck is fixed against horizontal translation

$$\sigma_s\leq\frac{GS_i}{A-B} \tag{8}$$

If the value A−B≤0, the bearing is stable and is not dependent on average compressive stress due to total load from applicable service load combinations (σ_s).

2.3.4 Reinforcement

Steel plate that is used to increase the vertical stiffness of SREI must provide certain conditions. The minimum thickness of steel reinforcement, h_s, shall be 1.5875 mm. The thickness of the steel reinforcement also shall satisfy

- At the service limit state $$h_s\geq\frac{3h_{ri}\sigma_s}{F_y} \tag{9}$$

- At the fatigue limit state $$h_s\geq\frac{2h_{ri}\sigma_L}{\Delta F_{TH}} \tag{10}$$

where ΔF_{TH} is constant amplitude fatigue threshold; σ_s average compressive stress due to total load from applicable service load combinations and σ_L average compressive stress at the service limit state (load factor=1.0) due to live load.

Fig. 2 Main page of SREI-CAD

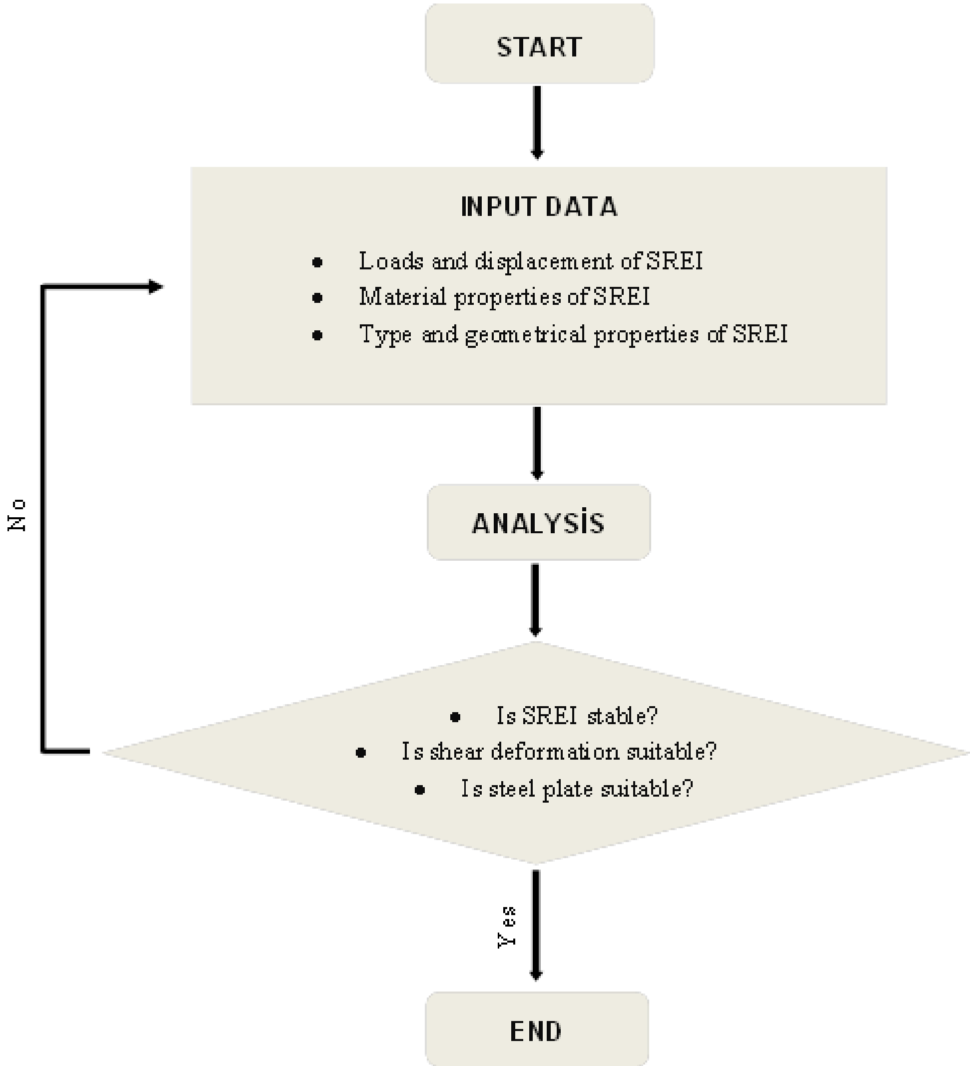

Fig. 3 Flow chart of SREI-CAD

Table 1 Properties of SREI

Properties of SREI		
Type	Circular	Rectangular
Dimension (mm)	*Φ*400	400*300
Thickness of interior rubber layer (mm)	12	
Number of rubber layer	5	
Thickness of exterior rubber layer (mm)	2.5	
Thickness of reinforcing steel plate (mm)	3	
Yield point of steel plate (MPa)	240	
Shear Modulus (MPa)	0,68	

Table 2 Loads and displacement data

Loads and displacement data	
Max. shear deformation (mm)	7.2
Max. vertical static load (N)	500000
Max. horizontal static load (N)	240000

3. Software of elastomeric bearing design

SREI is used many structures mostly in bridges. The connection between superstructure and substructure of the bridge is formed by SREI. Boundary conditions of the connection depend on geometrical and material properties of SREI. Considering its effects on structures dynamic behavior, the importance of accurate design of SREI is understood. The above design criteria of SREI according to AASHTO LRFD was integrated and implemented in computer software in order to facilitate the process and visualize the results in a useful way to the user. The main page and flow chart of software (SREI-CAD) is illustrated in Figs. 2 and 3, respectively.
With the help of using SREI-CAD, rectangular and circular types of isolator are analyzed and compared to each other. For this purpose dimension value of circular and rectangular isolator is selected 400*Φ* and 400*300, respectively. The aim of selecting these values is that getting surface area closer to each other. The other properties, load and displacement data given in Tables 1-2 is selected same in order to find the sole effect of isolator type on analysis results.

3.1 User input

The input menu of SREI-CAD consists of three main tabs named geometrical properties, loads and displacement and material properties. Firstly type of SREI is selected in geometrical properties tab and dimensional properties of selected SREI are entered. Geometrical properties tab of selected rectangular and circular SREI is illustrated in Figs. 4(a)-4(b), respectively.

Loads and displacement tab is illustrated in Fig. 5. Maximum shear deformation and exposed maximum static and live load is required for both SREI types. Horizontal displacement of the bridge is only visible for rectangular SREI. This additional information is needed for calculation of rectangular SREI's stability.

In material properties tab, shear and elastic modulus of SREI is required. In this tab software gives additional information with help text as shown in Fig. 6. There are two options as user-defined and default for shear and elastic modulus of SREI. If user has information about these properties, the user selects user-defined option and inputs the value of modulus. Otherwise, the user selects default options and the software selects appropriate shear modulus. Elastic modulus is calculated with Eq. (4) recommended by AASHTO LRFD.

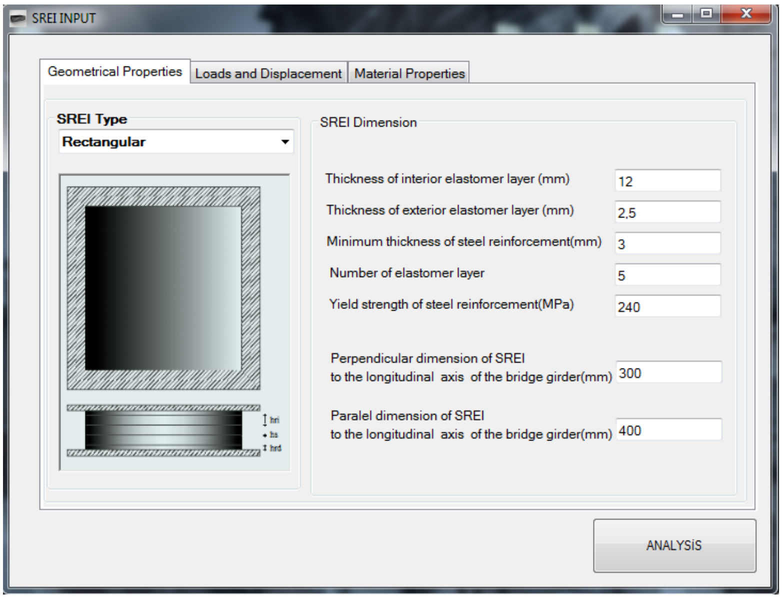

(a) Rectangular SREI

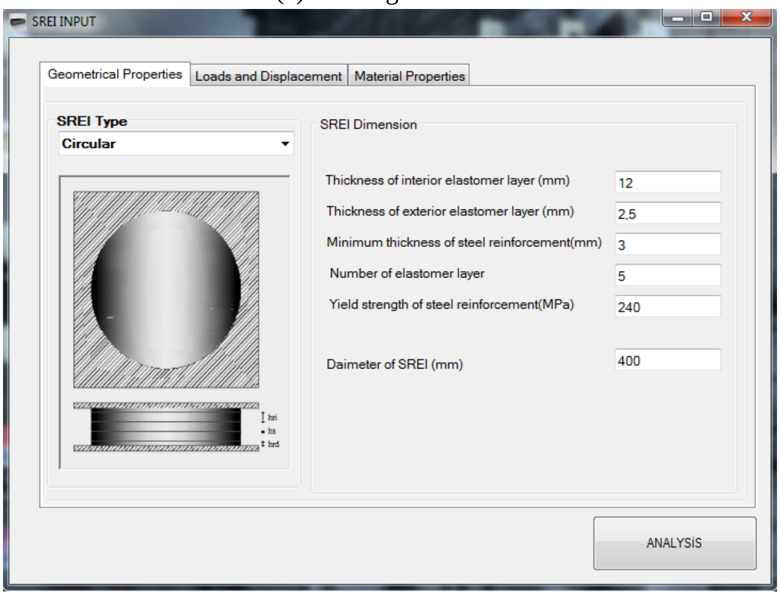

(b) Circular SREI

Fig. 4 Geometrical properties tab of SREI-CAD

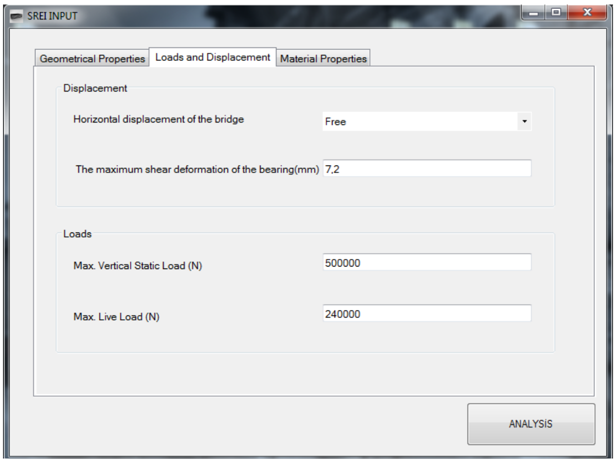

(a) Rectangular SREI

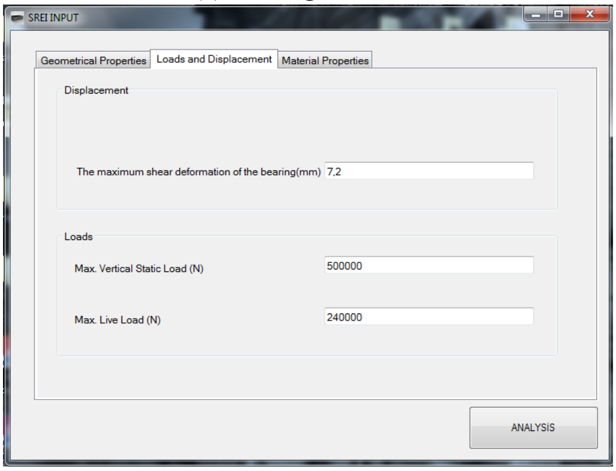

(b) Circular SREI

Fig. 5 Loads and displacement tab of SREI-CAD

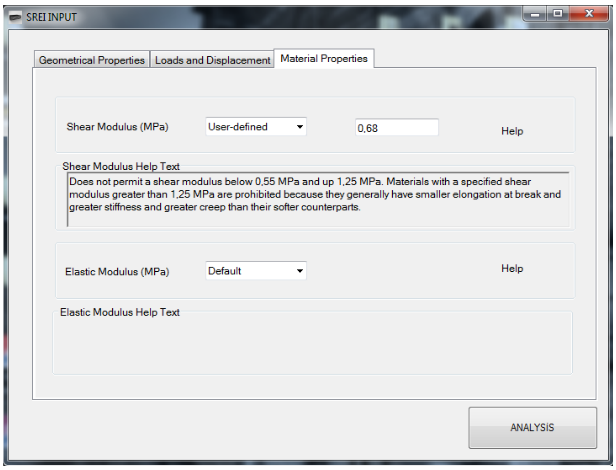

Fig. 6 Material properties tab of SREI-CAD

3.2 Output data

After entering input data as described above and clıcking ANALYSIS button, output data is obtained. The output menu of SREI-CAD consists of four main tab namely stability, steel plate, shear deformations and stiffness of SREI. Stability tab is illustrated in Fig. 7. In this tab, the value of stability parameters A, B and stability state of SREI is given. If selected SREI is not stable, i.e., the dimension of SREI isn’t adequate, the background color of rich text box turns red and the dimension of SREI has to be changed. For example, the rectangular bearing from the selected SREI provide the stability condition whereas circular bearing didn’t provide as shown in Figs. 7(a)-7(b) respectively.

Steel plate tab is illustrated in Fig. 8. In this tab the control of minimum steel plate thickness and thickness of steel plate under service and fatigue limit state is performed. As it is seen in the Fig. 8 selected circular and rectangular SREI are ensured all the requirements of steel plate.

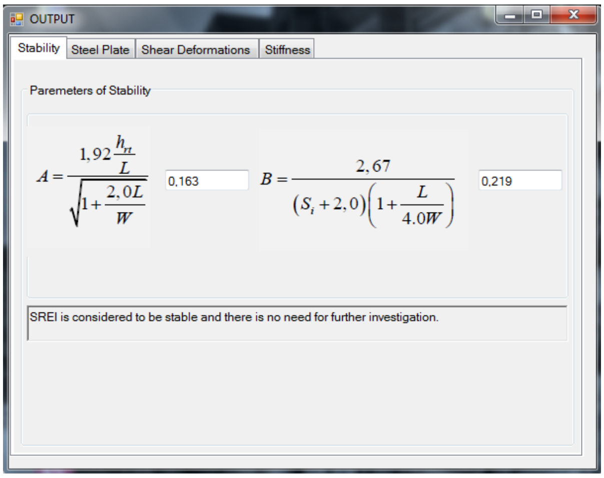

(a) Rectangular SREI

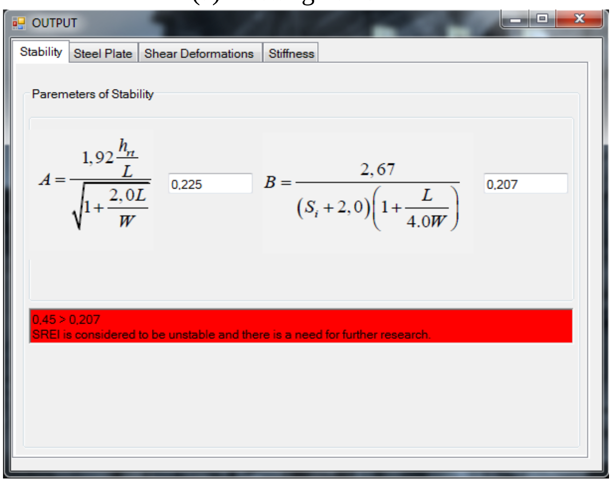

(b) Circular SREI

Fig. 7 Stability tab of SREI-CAD

Shear deformations tab is illustrated in Fig. 9. In this tab the control of total rubber thickness and shear deformation of SREI under combinations of axial load, rotation, and shear at the service limit state are performed. As it is seen in the Fig. 9 selected circular and rectangular SREI are ensured all the requirements for shear deformation.

Vertical, horizontal and rotational stiffnesses are given in the stiffness tab. As it is seen in the Fig. 10, the values of stiffness of selected circular and rectangular SREI are illustrated.

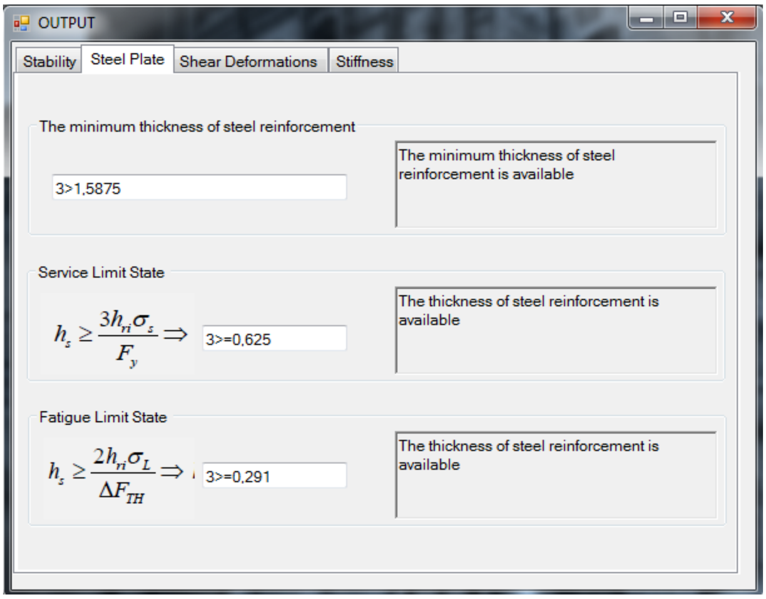

(a) Rectangular SREI

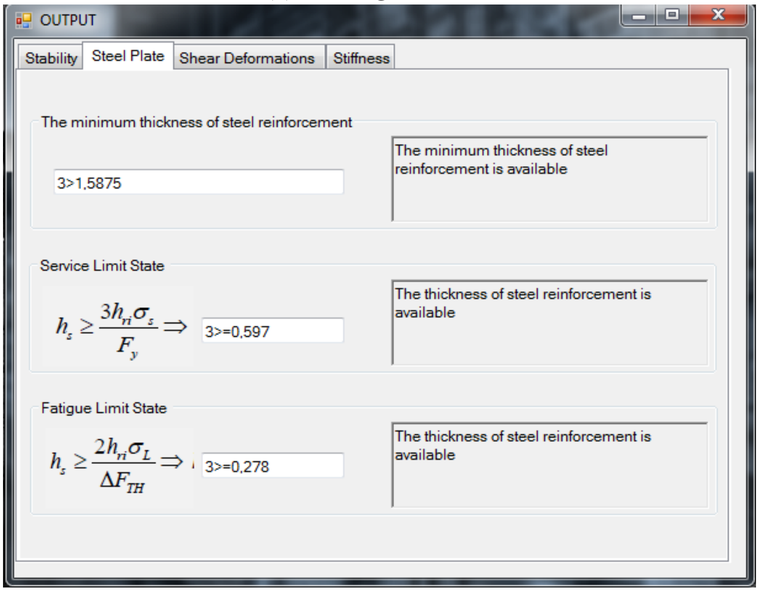

(b) Circular SREI

Fig. 8 Steel plate tab of SREI-CAD

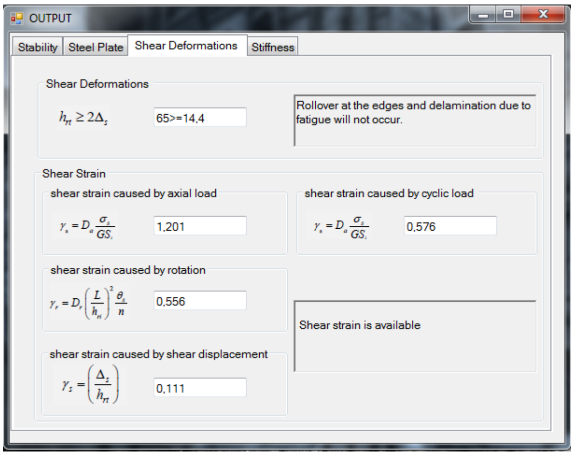

(a) Rectangular SREI

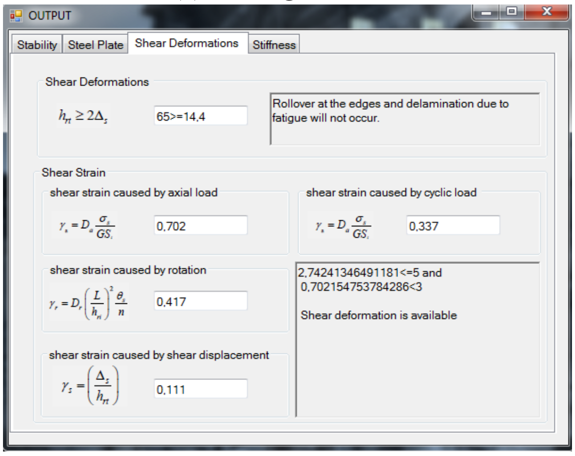

(b) Circular SREI

Fig. 9 Shear deformation tab of SREI-CAD

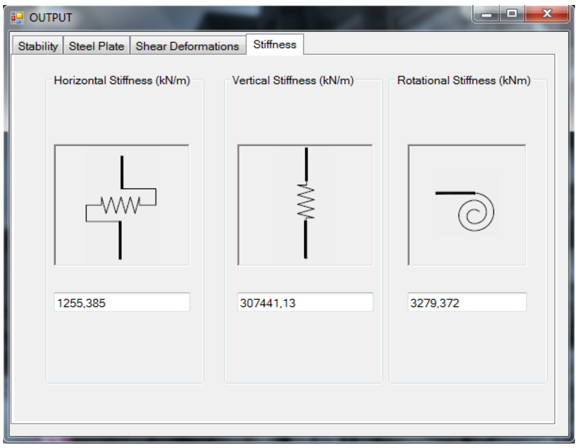

(a) Rectangular SREI

Fig. 10 Stifness tab

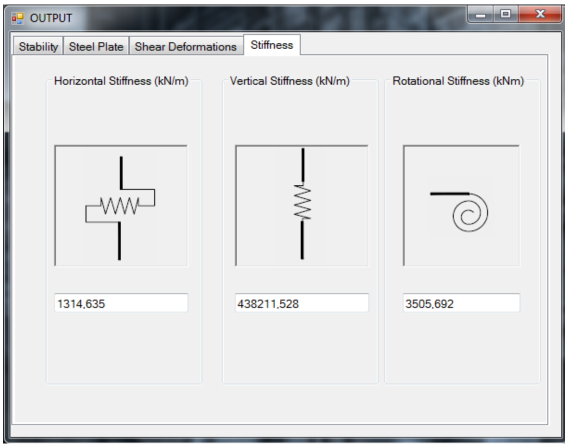

(b) Circular SREI

Fig. 10 Continued

4. Conclusions

This paper presents design procedure of steel elastomeric isolator (SREI) according to American Association for State Highway and Transportation Officials Load and Resistance Factor Design (AASHTO LRFD). Design procedure is also implemented in a software (SREI-CAD) written in C# programming language using Microsoft Visual Studio editor. The selection of SREI is complicated process includes satisfying all the design constraints arising from code provisions and maximizing performance at the lowest possible cost. Thanks to SREI-CAD the complicated and time consuming design process of rectangular or circular SREIs, subjected to different loads, having different cross-sections and material properties, are designed accurately in a short time The results taking from SREI-CAD is visualized in a user-friendly way to the user. In this paper, in order to find the sole effect of isolator type, circular and rectangular SREI which has similar properties, load and displacement conditions are selected. The properties of SREI, load and displacement data are entered to the software. The outputs of analysis which are stability, steel plate, shear deformations and stiffness visualized to the user. From the results of this study, the following observations can be made:

• To ensure the stability of circular elastomer bearing at the service limit state is generally complicated than rectangular bearing. Because, according to AASHTO LRFD there is an additional stability equation for rectangular SREI.

• To ensure the stability of rectangular SREI implemented fixed bridge deck against horizontal translation is easier than the bridge deck is free to translate horizontally.

• The maximum shear deformation of the bearing is controlled with total rubber thickness.

References

Akoglu, C. and Celik, O.C. (2008), “Effect of elastomerıc bearing modeling parameters on the seismic design of RC highway bridges with precast concrete girders”, *World Conference on Earthquake Engineering*, China, October.

American Association of State Highway and Transportation Officials (1961), *AASHTO LRFD bridge design specifications*, Washington, DC.

American Association of State Highway and Transportation Officials (2012), *AASHTO LRFD bridge design specifications*, Washington, DC.

Atmaca, B., Yurdakul, M. and Ateş, Ş. (2014), "Nonlinear dynamic analysis of base isolated cable-stayed bridge under earthquake excitations", *Soil Dyn. Earthq. Eng.*, **66**, 314-318.

Buckle, I.G. and Kelly, J.M. (1986), "Properties of slender elastomeric isolation bearings during shake table studies of a large-scale model bridge deck", *Joint Seal. Bear. Syst. Concrete Struct.*, American Concrete Institute, Detroit, Mich., **1**, 247-269.

Chen, Z., Zhao, H. and Lou, M. (2015), "Seismic performance and optimal design of framed underground structures with lead-rubber bearings", *Struct. Eng. Mech*., **58**(2), 259-276.

Danielle, L., Mariacristina, S. and Giorgio, S. (2014), "Optimal design of the seismic protection system for isolated bridges", *Earthq. Struct*., **6**(7), 969-999.

Forcellini, D. and Kelly, J.M. (2014), "Analysis of the large deformation stability of elastomeric bearings", *J. Eng. Mech.*, **140**(6), 04014036.

Green, T., Yazdani, N., Spainhour, L. and Cai, C.S. (2007), "Effect of bearing stiffness and skew angle on performance of precast concrete bridge", *Transport. Res. Record*, **1770**, 27-33.

Harper, Z.S. and Consolazio, G.R., (2013), "Calculation method for quantifying axial and roll stiffnesses of rectangular steel-reinforced elastomeric bridge bearing pads", *Transport. Res. Record*, **2331**, 3-13.

Islam, S., Hussain, R.R., Jumaat, M.Z. and Darain, K.M. (2014), "Implication of rubber-steel bearing nonlinear models on soft storey structures", *Comput. Concrete*, **13**(5), 603-619.

Jian, F., Xiaohong, L. and Yanping, Z. (2015), "Optimum design of lead-rubber bearing system with uncertainty parameters", *Struct. Eng. Mech*., **56**(6), 959-982.

Kim, D., Oh, J., Do, J. and Park, J. (2014), "Effects of thermal aging on mechanical properties of laminated lead and natural rubber bearing", *Earthq. Struct.*, **6**(2), 127-140.

Manos, G.C., Mitoulis, S.A. and Sextos, A.G. (2011), "Preliminary design of seismically isolated R/C highway overpasses - features of relevant software and experimental testing of elastomeric bearings", *III ECCOMAS Thematic Conference on Computational Methods in Struct. Dynamics and Earthquake Engineering*, Corfu, Greece, May.

Melkumyan, M.G. (2013), "New approach in design of seismic isolated buildings applying clusters of rubber bearings in isolation systems", *Earthq. Struct*., **6**(4), 587-606.

Moon, B.Y., Kang, G.J., Kang, B.S. and Kelly, J.M. (2002), "Design and manufacturing of fiber reinforced elastomeric isolator for seismic isolation", *J. Mater. Proc. Technol*., **130**(131), 145-150.

Muscarella, J.P. (1995), "An experımental study of elastomerıc bridge bearings with design recommendations", Degree of Doctorate of Philosophy, Civil Engineering Department, The University of Texas at Austin, USA, August.

Olmos, B.A. and Roesset J.M. (2010), "Effects of the nonlinear behavior of lead-rubber bearings on the seismic response of bridges", *Earthq. Struct*., **2**(1), 215-230.

Patrick, L.Y., Azlan, A., Ahmad, B.A., Rahman and Abdul, K.M. (2014), "Seismic base isolation of precast wall system using high damping rubber bearing", *Earthq. Struct*., **6**(7), 1141-1169.

Roeder, C.W., Stanton, J.F. and Taylor, A.W. (1987), "Performance of elastomeric bearings", National Cooperative Highway Research Program Report #298, Transportation Research Board, National Research Council, Washington, DC.

Yazdani, N., Eddy, S.M. and Cai, C.S. (2000), "Validation of AASHTO bearing stiffness for standard precast concrete bridge girders", *ACI Struct. J.*, **97**(3), 436-443.

TK